POLITECNICO DI TORINO
Repository ISTITUZIONALE

SNO-Based Design of Wide-Angle Beam-Scanning Reflectarrays

Original
SNO-Based Design of Wide-Angle Beam-Scanning Reflectarrays / Beccaria, M., Niccolai, A., Massaccesi, A., Zich, R.E., Pirinoli, P.. - In: RADIO SCIENCE LETTERS. - ISSN 2736-2760. - ELETTRONICO. - 2:(2020), pp. 1-5. [10.46620/20-0047]

Availability:
This version is available at: 11583/2866692 since: 2021-02-15T17:42:22Z

Publisher:
URSI Publication

Published
DOI:10.46620/20-0047

Terms of use:

This article is made available under terms and conditions as specified in the corresponding bibliographic description in the repository

Publisher copyright

(Article begins on next page)

07 October 2026

SNO-based Design of Wide-angle Beam-scanning Reflectarrays

M. Beccaria, A. Niccolai, A. Massaccesi, R.E. Zich, P. Pirinoli

Abstract – In this letter, the design of a passive Reflectarray (RA) with beam-scanning capabilities over a wide scan range is addressed. The proposed approach is based on the use of an efficient Evolutionary Algorithm (EA), the Social Network Optimization (SNO), and by the definition of a proper optimization environment which allows the simultaneous optimization of the antenna radiation pattern for different pointing directions, keeping under control the computational cost of the procedure. The effectiveness of the method is validated through the experimental characterization of a prototype, whose performance is also compared with that of a conventional bifocal configuration.

1. Introduction

Nowadays, many applications require the use of a beam-scanning antenna; among the possible solutions for their realization, also Reflectarrays (RAs) have been considered, in view of their interesting features when adopted to design fixed beam antennas [1], [2].

The most straightforward way to obtain a beam-scanning RA is that of introducing active elements, as varactors, pin-diodes or MEMS [3-6]: the resulting antenna performance is good, but its complexity significantly increases. An alternative is that of using a passive reflectarray and to steer the beam direction either moving the feed along a circular arc to keep constant the distance with the RA surface, either using a feed array [7-11]: the absence of active elements reduces the RA design complexity, but at a cost of a degradation of the antenna radiation patterns, characterized by the enlargement of the main beam, the increasing of the Side Lobe Level (SLL) and the decreasing of the maximum gain.

To overcome this problem, different techniques were proposed, as that of designing a "bifocal" reflectarray [11], whose performance can be eventually enhanced using a double reflector configuration [12]. or the use of the Phase Matching Method (PMM) [8]. An alternative solution consists in exploiting global Evolutionary Algorithms (EAs) even if their application to the optimization of a RA is still a challenging issue for the following reasons: (a) the number of variables involved in the process is generally great, since they correspond to the degrees of freedom of the RA unit cells by the number of cells, (b) the mathematical function that models the problem is

computationally expensive or not accurate enough, and therefore there is (c) the risk that the stochastic nature of the method provides a solution that behaves in a completely different way from the one predicted by the optimizer. Despite of these drawbacks, in [13-17], some results on the use of the most popular EAs, as the Genetic Algorithm (GA), the Particle Swarm Optimization (PSO) and the Differential Evolution (DE) for the optimization of shaped-beam, not uniformly spaced or multi-beam reflectarrays were presented.

In this letter, a more recent algorithm, the Social Network Optimization (SNO), that has shown very good performance when used for the design of flat [18] or shaped [19] beam reflectarrays, is applied to the design of a wide-angle, beam-scanning RA, covering a scan range from -40° to +40°. Particular care is devoted to the definition of the optimization environment, designed to guarantee accurate and reliable results and to minimize the process numerical cost. Some very preliminary results were already presented in [20,21], where the performance of the SNO, and especially its convergence capability, was compared with that of another family of efficient EAs, the M_mC_n-BBO [22], an enhanced version of the Biogeography-Based Optimization (BBO) [23]. Here, the effectiveness of the SNO is assessed by the experimental characterization of a prototype, designed using the optimization algorithm, and the comparison between its performance and that of an equivalent bifocal RA.

The main features of the SNO are summarized in the next section, while in Sect. 3 the considered problem and the related optimization environment are described. Finally, in Sect. 4 the performance of the optimized reflectarray is discussed and compared with that of the bifocal solution.

2. The Social Network Optimization

SNO is a population-based algorithm that mimics the information sharing process on online Social Networks. The population of the algorithm consists in the users of the considered social network that share their ideas and interact online. Each user is characterized by its opinion that is shared by means of a post (out of the metaphor, the candidate solution of the optimization problem). The post is evaluated by the social network and it receives a visibility value (the cost value of the problem) that indicates how much it is probable that another user can read it and can be influenced by it.

The online interaction takes place through two different networks: the friend one, characterized by strong connections among users and by a slow evolution rate, and the trust network, characterized by weaker interactions and by an evolution based on the posts' visibility value. Each user exchanges opinions with other individ-

uals being influenced by both the networks. The interaction is based on the following equation:

$$\mathbf{o}(t+1) = \mathbf{o}(t) + \alpha[\mathbf{o}(t) - \mathbf{o}(t-1)] + \beta[\mathbf{a}(t) - \mathbf{o}(t)] \quad (1)$$

where **o** is the user opinion and **a** is the attracting idea, obtained by means of a single point crossover from the ideas deriving from the two networks.

The SNO was compared with the GA and the PSO, through their application to several benchmark functions that are widely used for EAs testing, since each of them has unique features useful to measure the algorithms performance on different scenarios. More details on these functions and their complete mathematical formulation can be found in [24]. In Table 1, the average cost value obtained by application of the three algorithms to the listed benchmark functions, after 5,000 objective function calls and considering 50 independent trials, is reported. In most of the cases (the values in the colored cells are the best results for each function) the SNO outperforms the other two algorithms, and this confirms its good features.

Table 1: Comparison between GA, PSO and SNO.

Function	*GA*	*PSO*	*SNO*
Ackley	2.4	3	0.99
Griewank	1.63	1.27	1.17
Penalty 1	0.56	5.32	0.19
Rastrigin	71.59	143.11	8.91
Rosenbrock	23.17	19.36	40.96
Schwefel-221	4.52	13.29	10.36
Sinc-N	0.73	1	0.09
Sphere	0.18	0.07	0.05

3. The optimization environment

The optimization problem addresses the design of a RA with $N \times N$ unit cells, showing scanning capabilities over the range $[\theta^s_{min}, \theta^s_{max}]$ in the elevation plane. The problem is intrinsically multi-objective, but to keep under control the computational cost, still guaranteeing good convergence and reliability, a proper cost function that is the linear combination of different terms, each representing a specific objective, was introduced:

$$C(\mathbf{d}, S_i) = \sum_{i \in S} \lambda_i \cdot (c_1(\mathbf{d}, S_i) + c_2(\mathbf{d}, S_i)) \quad (2)$$

In eq.2, **d** is the vector of variables used to control the optimization process, λ_i are scalar coefficients and S is

the set of directions of maximum radiation considered, during the optimization, within the scan coverage.

The c_1 function is defined as the integral of the error Δ_{S_i} between the radiation pattern evaluated with the Aperture Field Method (AFM) [1] and the values of the optimization variables provided by the SNO, and a predefined 3D mask:

$$c_1(\mathbf{d}, S_i) = \iint \Delta_{S_i}(\theta, \phi) d\theta d\phi \tag{3}$$

while c_2 represents the scan angle error $\Delta\theta_{S_i}$, i.e. the squared value of the difference between the desired direction of maximum radiation θ_s and the actual one, θ_{max},

$$c_2(\mathbf{d}, S_i) = \Delta\theta_{S_i} = \left[(\theta_{S_i} - \theta_{max}) \frac{180}{\pi} \right]^2 \tag{4}$$

and was introduced to speed up the algorithm convergence and to guarantee that it properly finds the direction of maximum radiation.

The variables collected in the vector $\mathbf{d}$ are of two types: 1) the free geometrical parameters characterizing each unit cell and 2) the Beam Deviation Factor (BDF), i.e. the ratio between θ_{max} and the angle of incidence θ_{inc} between the impinging field and the direction orthogonal to the RA surface. A BDF is associated to each considered direction of maximum radiation. Since they have different domains of definition, variables normalized in the range [0; 1] are used.

To improve the effectiveness of the SNO and to guide it to find a feasible solution, the available information about the physics of the considered problem is implemented in the optimization environment. In particular, the masks used in correspondence of the different pointing directions are not equal, to take into account that the beam steering affects the radiation patterns, with a widening of the main beam and an increase of the SLL. Moreover, a symmetrical scan coverage can be obtained with a symmetrical distribution of the unit cells: this means that only half of the scanning range can be considered during the optimization, and also that the symmetries can be used to reduce the size of the problem, i.e. the computational time for its solution.

4. Results

In the considered example, $N = 24$ and each unit cell has a size equal to $\lambda/2$, at $f_0 = 30$ GHz, for a total size of the square RA aperture of $12\lambda \times 12\lambda$. The radiating elements are square patches, printed on a Diclad® 527 substrate with a thickness of 0.8 mm and $\varepsilon_r = 2.55$; the phase of the unit cell reflection coefficient is controlled through the patch side W [19]. The aperture is illuminated by a smooth wall horn whose radiation pattern can be modeled as a $[cos(\theta)]^q$ with $q = 12.5$ [25]. The focal

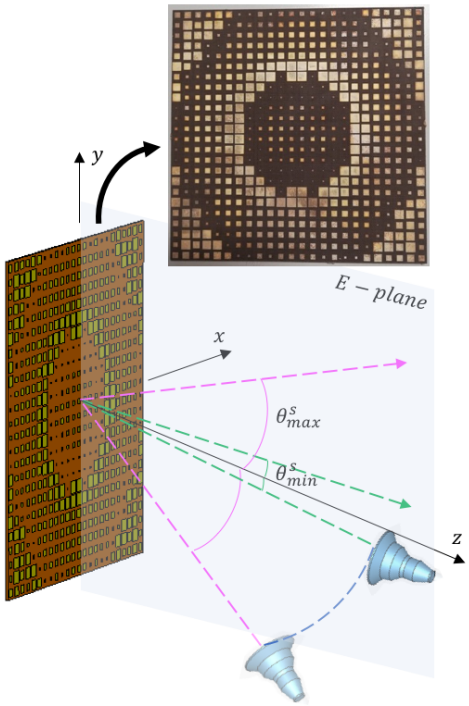

Figure 1: Sketch of the antenna configuration, with two positions of the feed, corresponding to the direction of maximum radiation characterized by θ^s_{min} and θ^s_{max}; photo of prototype of the RA designed with the SNO.

distance from the phase center of the feed to the aperture is $f/D = 1.2$, to reduce the taper. A sketch of the resulting configuration is shown in Fig.1.

The RA total number of degrees of freedom is equal to $N^2 = 576$, but, considering the symmetries in the patches distribution, it reduces to $N_{DF} = 144$. Moreover, only the positive half scan range is considered in the optimization: as a consequence, θ^s_{max} was chosen equal to 40°, while $\theta^s_{min} = 10°$, to avoid radiation in the broadside direction that would be affected by the blockage introduced by the feed. In this interval, four directions of maximum radiation, i.e. θ_{max} =10°, 20°, 30°, 40° were considered in the optimization process; therefore, the total number of optimization variables is $N_{DF}+4$ BDF. The starting position of the feed is specular to the direction of maximum radiation of the RA identified by θ^s_{min}; then the feed is moved along a circular arc to cover the scanning range up to θ^s_{max}, (see Fig. 1).

The termination criterion adopted for the optimization is 50,000 objective function calls; the average value of the curves of convergence and the corresponding standard deviation obtained considering 40 independent trials are plotted in Fig. 2: they prove the good convergence capability of the process and also its reliability.

The radiation patterns obtained at the end of the

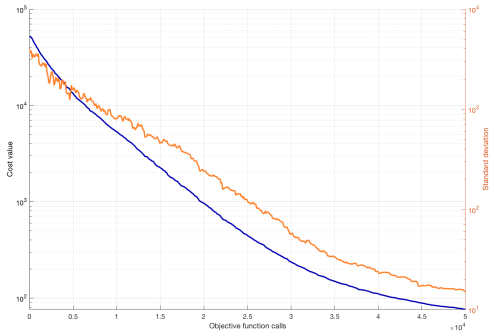

Figure 2: Average value of the curves of convergence (–) and corresponding standard deviation (–).

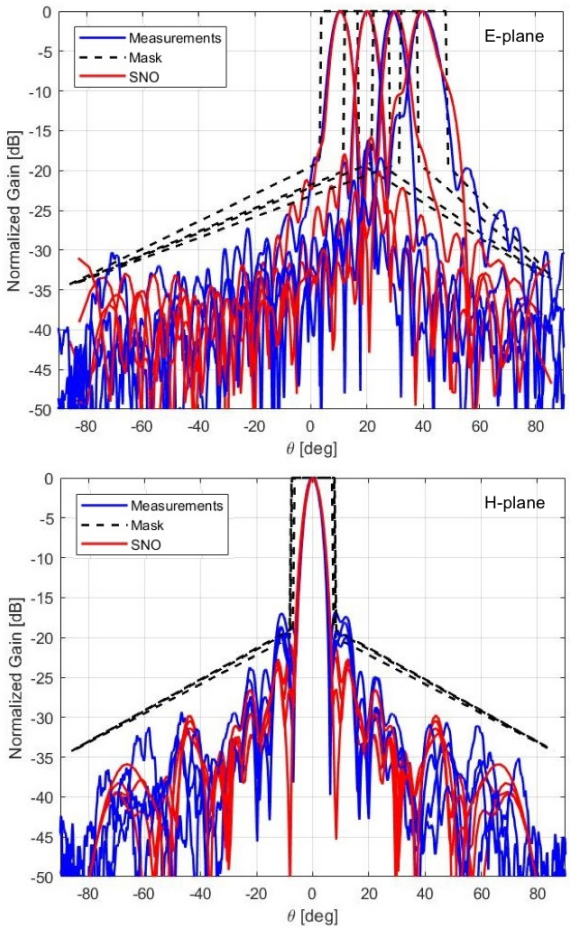

Figure 3: Optimized RA: normalized radiation patterns at the end of the optimization process (–) and measured ones (–) in the E-plane (top) and in H-plane (bottom) for the pointing directions in the E-plane θ_{max} =10°, 20°, 30°, 40°; masks adopted during the optimization process (– –).

process in the four considered directions of maximum radiation in the E and H planes are plotted in Fig. 3, together with the adopted masks. In the same figure, also the measured patterns relative to the prototype shown in the inset of Fig. 1, are shown. It can be noticed the good agreement between the results obtained at the end of the optimization and the measured ones, and, above all, that they satisfy the masks almost everywhere: this proves the effectiveness of the developed technique and the beam-scanning capability of the RA. Note that the radiation patterns for the negative part of the scan range are not shown, since they are symmetrical to the plotted ones.

To further validate the efficiency of the proposed method, the RA performance is compared with that of a bifocal configuration, with the same size, designed to compensate the average of the phase maps needed to have maximum radiation for $\theta_{max} = \pm 40^{\circ}$. The measured radiation patterns in the two principal planes for the resulting configuration are plotted in Fig. 4, together with those for the optimized RA. Also in this case, in the E-plane only the radiation patterns for positive scanning angles are shown. The quality of the optimization process is clear: the radiation patterns of the optimized configuration are characterized by narrower main beams and lower SLLs. Finally, in Fig. 5, the variation of the gain with the scanning angle is reported, for both the optimized and the bifocal reflectarrays. The continuous lines represent the evaluated gain, while the circles the measured values. These results confirm that the optimized RA outperforms the bifocal one: the maximum gain that occurs almost for the same angle, is 2 dB higher, at a cost of a slightly larger variation of the gain over the considered subrange, that is equal to $\Delta G = 2$ dB for the SNO solution and $\Delta G = 1.7$ dB for the bifocal one.

5. Conclusions

In this letter, the design of a beam-scanning passive reflectarray antenna, carried out with a promising Evolutionary Optimization, Social Network Optimization, is presented, together with the description of the optimization environment developed to maximize the optimization efficiency and the accuracy and reliability of the obtained solution. Those features are proven through the experimental characterization of a prototype and the comparison of its performance with that of a bifocal RA.

6. Acknowledgement

The authors would like to thank Gianluca Dassano from the Politecnico di Torino for his valuable help in the experimental characterization of the antenna prototypes.

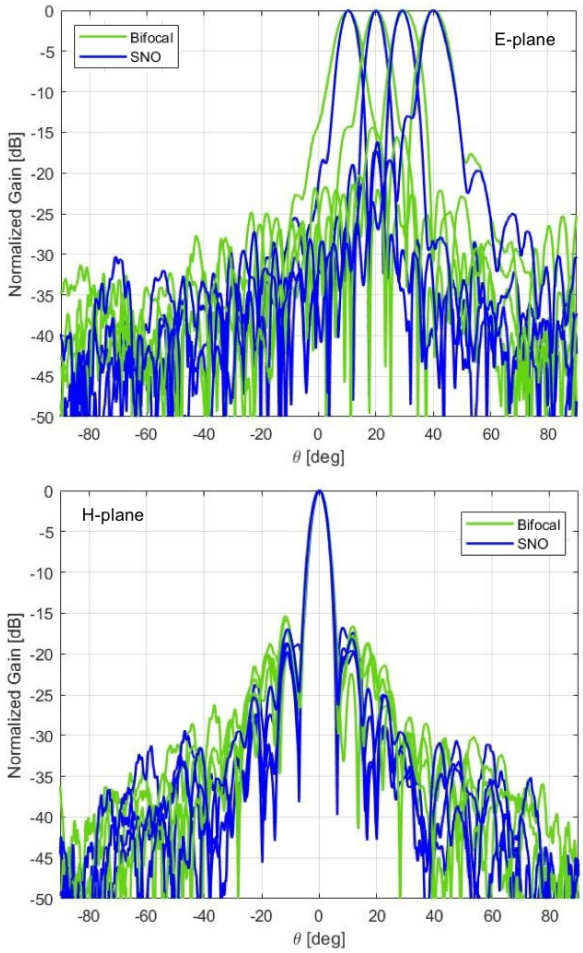

Figure 4: Measured normalized radiation patterns in the E-plane (top) and in the H-plane (bottom) for the pointing direction in the E-plane θ_{max} =10°, 20°, 30°, 40°: optimized RA (–); bifocal RA (–)

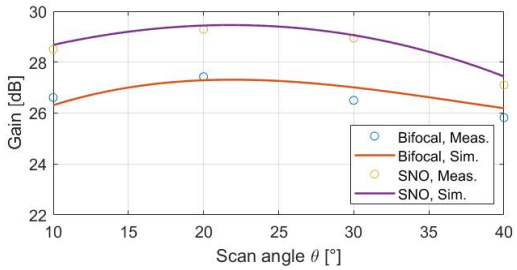

Figure 5: Variation of the gain as a function of the scan angle, for the optimized RA and the bifocal RA: evaluated values (–); measured values(o).

7. References

1. J. Huang and J.A. Encinar, *Reflectarray Antennas.* Wiley-IEEE press, 2008.

2. P. Nayeri, F. Yang, and A. Z. Elsherbeni, *Reflectarray Antennas: Theory, Designs, and Applications.* Wiley-IEEE press, 2018.
3. S. V. Hum, M. Okoniewski, and R. J. Davies, "Modeling and Design of Electronically Tunable Reflectarrays", *IEEE trans. on Antennas and Propag.*, vol. 55, no. 8, pp. 2200–2210, 2007.
4. M. Riel and J.-J. Laurin, "Design of an Electronically Beam Scanning Reflectarray using Aperture-Coupled Elements", *IEEE trans. on Antennas and Propag.*, vol. 55, no. 5, pp. 1260–1266, 2007.
5. E. Carrasco, M. Barba, and J.A. Encinar, "X-band Reflectarray Antenna with Switching-Beam using PIN Diodes and Gathered Elements", *IEEE trans. on Antennas and Propag.*, vol. 60, no. 12, pp. 5700–5708, 2012.
6. O. Bayraktar, O. A. Civi, and T. Akin, "Beam Switching Reflectarray Monolithically Integrated with RF MEMS Switches", *IEEE trans. on Antennas and Propag.*, vol. 60, no. 2, pp. 854–862, 2011.
7. P. Nayeri, F. Yang, and A. Z. Elsherbeni, "Beam-Scanning Reflectarray Antennas: A Technical Overview and State of the Art", *IEEE Antennas and Propag. Magazine*, vol. 57, no. 4, pp. 32–47, 2015.
8. G.-B. Wu, S.-W. Qu, and S. Yang, "Wide-Angle Beam-Scanning Reflectarray with Mechanical Steering", *IEEE Trans. on Antennas and Propag.*, vol. 66, no. 1, pp. 172–181, 2017.
9. X. Yang, S. Xu, F. Yang, M. Li, H. Fang, Y. Hou, S. Jiang, and L. Liu, "A Mechanically Reconfigurable Reflectarray with Slotted Patches of Tunable Height", *IEEE Antennas and Wireless Propag. Letters*, vol. 17, no. 4, pp. 555–558, 2018.
10. P. Mei, S. Zhang, and G. F. Pedersen, "A Low-Cost, High-Efficiency and Full-Metal Reflectarray Antenna with Mechanically 2-D Beam-Steerable Capabilities for 5G Applications", *IEEE Trans. on Antennas and Propag.*, 2020.
11. P. Nayeri, F. Yang and A.Z. Elsherbeni, "Bifocal Design and Aperture Phase Optimizations of Reflectarray Antennas for Wide-Angle Beam Scanning Performance", *IEEE Trans. on Antennas and Propag.*, vol. 61, no. 9, pp. 4588–4597, 2013.
12. E. Martinez-de-Rioja, J. A. Encinar, R. Florencio and C. Tienda, "3-D Bifocal Design Method for Dual-Reflectarray Configurations with Application to Multibeam Satellite Antennas in Ka-Band", *IEEE Trans. on Antennas and Propag.*, vol. 67, no. 1, pp. 450–460, 2018.
13. H. Yang, F. Yang, S. Xu, Y. Mao, M. Li, X. Cao, and J. Gao, "A 1-bit 10×10 Reconfigurable Reflectarray Antenna: Design, Optimization, and Experiment", *IEEE Trans. on Antennas and Propag.*, vol. 64, no. 6, pp. 2246–2254, 2016.
14. Y. Aoki, H. Deguchi, and M. Tsuji, "Reflectarray with Arbitrarily-Shaped Conductive Elements Optimized by Genetic Algorithm", *2011 IEEE Int. Symposium on Antennas and Propag. (APSURSI)*, 2011, pp. 960-963.
15. D. Kurup, M. Himdi, and A. Rydberg, "Design of an Unequally Spaced Reflectarray", *IEEE Antennas and Wireless Propag. Letters*, vol. 2, pp. 33–35, 2003.

16. P. Nayeri, F. Yang, and A. Z. Elsherbeni, "Design of Single-Feed Reflectarray Antennas with Asymmetric Multiple Beams using the Particle Swarm Optimization Method", *IEEE Trans. on Antennas and Propag.*, vol. 61, no. 9, pp. 4598–4605, 2013.
17. C. Geaney, J. Sun, S. V. Hum, E. S. Rogers, E. Martinez-de-Rioja and J. A. Encinar, "Synthesis of a Multi-Beam Dual Reflectarray Antenna using Genetic Algorithms", *2017 IEEE Int. Symposium on Antennas and Propag. & USNC/URSI Nat. Radio Science Meeting*, San Diego, CA, 2017, pp. 1179–1180.
18. A. Niccolai, X. Pan, P. Pirinoli, F. Yang, R. E. Zich and S. Xu, "Flat Beam Optimization of 1-bit Reflectarray by means of Social Network Optimization", *2018 IEEE Int. Symposium on Antennas and Propag. & USNC/URSI Nat. Radio Science Meeting*, Boston, MA, 2018, pp. 543–544.
19. A. Niccolai, R.E. Zich, M. Beccaria and P. Pirinoli, "SNO Based Optimization for Shaped Beam Reflectarray Antennas", *2019 13th European Conf. on Antennas and Propag. (EuCAP)*, Krakow, Poland, 2019, pp. 1–4.
20. M. Beccaria, A. Massaccesi, P. Pirinoli, A. Niccolai and R.E. Zich, "SNO and mBBO Optimization Methods for Beam Scanning Reflectarray Antennas", *2019 IEEE Int. Symposium on Antennas and Propag. & USNC/URSI Nat. Radio Science Meeting*, Atlanta, GA, 2019, pp. 1037–1038.
21. A. Niccolai, M. Beccaria, A. Massaccesi, R.E. Zich and P. Pirinoli, "Optimization of Beam Scanning Reflectarray using $M_Q C_{10}$-BBO and SNO Algorithms", *2019 Int. Conf. on Electromagnetics in Advanced Applic. (ICEAA)*, Granada, Spain, 2019, pp. 0506–0509.
22. P. Pirinoli, A. Massaccesi, and M. Beccaria, "Application of the $M_m C_n$-BBO Algorithms to the Optimization of Antenna Problems", *2017 Int. Conf. on Electromagnetics in Advanced Applic. (ICEAA)*, Verona, Italy, 2017, pp. 1850–1854.
23. D. Simon, "Biogeography-based Optimization", *IEEE Trans. on Evol. Computation*, vol. 12, no. 6, pp. 702–713, 2008.
24. D. Simon, *Evolutionary Optimization Algorithms*, John Wiley & Sons, 2013.
25. M. Beccaria, G. Addamo, P. Pirinoli, M. Orefice, O. Peverini, G. Virone, D. Manfredi, and F. Calignano, "Feed system optimization for convex conformal reflectarray antennas", *2017 IEEE Int. Symposium on Antennas and Propag. & USNC/URSI Nat. Radio Science Meeting*, San Diego, CA, 2017, pp. 1187–1188.

A. Niccolai and R.E. Zich are with Dip. di Energia, Politecnico di Milano, Via La Masa 34, 20156 Milano; e-mail: alessandro.niccolai@polimi.it, riccardo.zich@polimi.it.

M. Beccaria, A. Massaccesi and P. Pirinoli are with Dept of Electronics and Telecommunications, Politecnico di Torino, Corso Duca degli Abruzzi 24, 10129 Torino, Italy; e-mail: michele.beccaria@polito.it, andrea.massaccesi@polito.it, paola.pirinoli@polito.it.